

COMPUTATIONAL INVESTIGATION OF HELICAL TRAVELING WAVE TUBE TRANSVERSE RF FIELD FORCES

Carol L. Kory, *Senior Member, IEEE*

ANALEX Corporation

NASA Lewis Research Center

21000 Brookpark Road, MS 54-5

Cleveland, Ohio 44135

(216) 433-3512 Fax: (216) 433-8705

and

James A. Dayton, Jr., *Fellow, IEEE*

Electron Dynamics Division

Hughes Telecommunications and Space Company

3100 W. Lomita, Torrance, CA 90509-2999

ABSTRACT

In a previous study using a fully three-dimensional (3D) helical slow-wave circuit cold-test model it was found, contrary to classical helical circuit analyses, that transverse RF electric fields have significant amplitudes compared with the longitudinal component. The RF fields obtained using this helical cold-test model have been scaled to correspond to those of an actual TWT. At the output of the tube, RF field forces reach 61%, 26% and 132% for radial, azimuthal and longitudinal components, respectively, compared to radial space charge forces indicating the importance of considering them in the design of electron beam focusing.

INTRODUCTION

A critically important component in helical traveling wave tubes (TWT's) is the focusing structure which keeps the electron beam from diverging and intercepting the slow-wave circuit. Interception between electron beam and RF circuit can result in excessive circuit heating and decreased efficiency, while excessive growth in the beam diameter can lead to backward wave oscillations and premature saturation, implying a serious reduction in tube performance. Electron optics codes used for designing beam focusing are typically based on balancing diverging forces due to space charge fields, beam rotation, and transverse velocity components due to thermal effects at the cathode and scattering from the electron gun grid. RF field defocusing forces generated by the helical slow-wave circuit are neglected, and until recently it was impossible to accurately represent these helical fields because of the complexity of the circuit.

It has been demonstrated in [1] that using the simulation code, MAFIA (Solution of **MA**xwell's equations by the **FI**nite-**I**ntegration-**A**lgorithm) [2, 3], cold-test helical structures can be accurately modeled with actual tape width and thickness, dielectric support rod geometry and materials. Of the nine modules included in the MAFIA code, results of this report were calculated using the M (mesh generator), E (eigenmode solver) and P (postprocessor).

The accurate 3D helical cold-test model was used to investigate standard approximations in the analysis of helical traveling-wave tube measured interaction impedance by Lagerstrom [4]. The most prominent approximations in his analysis were addressed and it was found that several are in significant error [5]. In particular, it was found that helical RF transverse electric fields have significant amplitudes relative to the longitudinal component. The forces due to these transverse fields may significantly affect beam behavior. This is especially a concern near the output of the tube where RF fields have grown substantially due to transfer of energy from the electron beam. To investigate the significance of RF field forces on electron beam behavior, an analysis was completed and is reported on here comparing these RF forces to radial space charge forces near the TWT output.

The TWT used as a model is a 40 Watt, 18-40 GHz TWT for the millimeter-wave power module (MMPM) [6]. The experimental helix slow-wave circuit includes rectangular, tungsten, helical tape supported by T-shaped BeO rods inside a conducting barrel as shown for the end view in Figure 1. The operating parameters for the tube are shown in Table I. The specific results presented here apply only to the mentioned TWT; however, these results can serve as a general guide for similar devices, and the computational techniques are readily applicable to other TWT's.

The concept of RF defocusing fields is not new and has been observed by several investigators [7, 8, 9, 10, 11 and 12]. However, previous work has been based on greatly simplified models or limited experimental measurements. To obtain unrestricted information regarding transverse RF fields, an accurate 3D helical model is necessary, and this has not been available until recently.

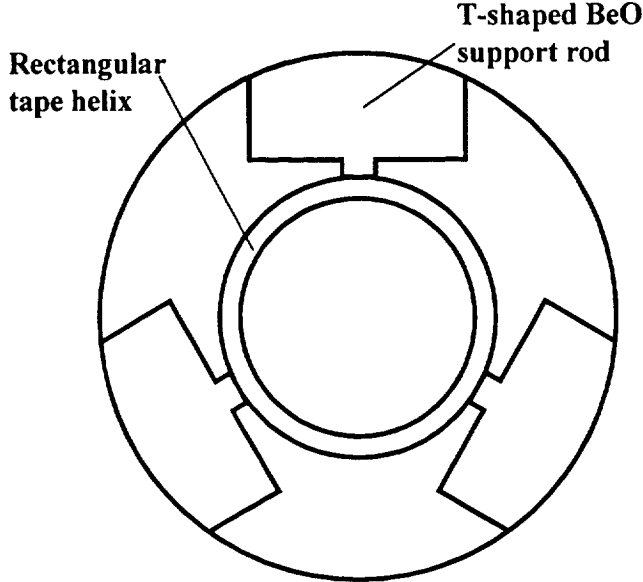


Figure 1 Hughes MPPM helical slow-wave circuit

Table I Operating parameters for the Hughes 8916H helical TWT

| | |
|-----------------|------|
| Frequency (GHz) | 26.0 |
| V_o (kV) | 7.6 |
| I_o (mA) | 81.0 |
| P_{in} (dBm) | 14.0 |
| P_{out} (dBm) | 46.6 |

SIMULATION AND ANALYSIS

The helical circuit is simulated using MAFIA by modeling one helical turn with resolution of 36 x 115 x 48 mesh units in the radial, azimuthal and axial directions, respectively.

The quasi-periodic boundary condition is applied at the longitudinal ends, permitting the user to choose a fixed phase advance per turn in the axial direction and allowing the frequency to be obtained at any axial phase shift. The azimuthal electric field amplitudes at the beam radius, b , and $\theta = 0$, obtained using MAFIA and normalized to the maximum value of longitudinal electric field are plotted in Figure 2 versus longitudinal distance for the Hughes MMPM helical TWT slow-wave circuit. The beam radius is assumed to be half of the helix average radius ($b = a/2$). From the plot, it can be seen that E_θ is nontrivial, amounting to about 10% of E_{zmax} at $\beta L = 30$ degrees (8.75 GHz) and about 30% at $\beta L = 150$ degrees (42.26 GHz).

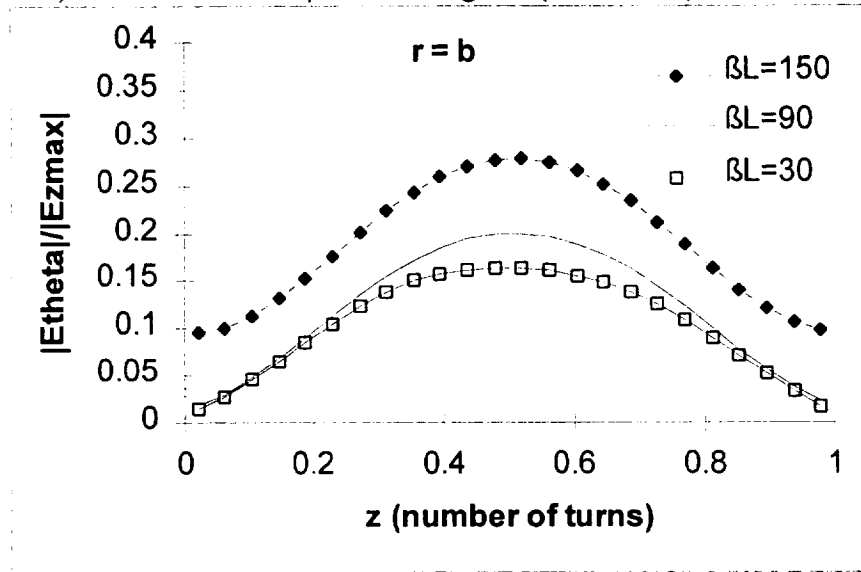


Figure 2 Azimuthal electric field amplitude normalized to the maximum value of longitudinal electric field as a function of z at $r=b$ and $\theta = 0$

The radial field amplitudes at the beam radius and $\theta = 0$, normalized to the maximum value of longitudinal electric field are plotted in Figure 3 versus longitudinal distance. From the plot, it can be seen that E_r is nontrivial, amounting to about 30% of E_{zmax} at $\beta L = 30$ degrees (8.75 GHz) and about 68% at $\beta L = 150$ degrees (42.26 GHz).

As an estimate of the effect that the azimuthal and radial electric fields have on defocusing the electron beam, a comparison of RF transverse field forces to radial space charge forces has been completed. The eigenmode solver of MAFIA uses an arbitrary excitation level; thus, electric fields in Figure 2 and Figure 3 must be scaled to the TWT operating parameters of interest. The defocusing effect of RF fields at the input of the tube will be negligible, thus we focus on the output. The scale factors between simulated and actual RF fields at the tube output are derived as follows.

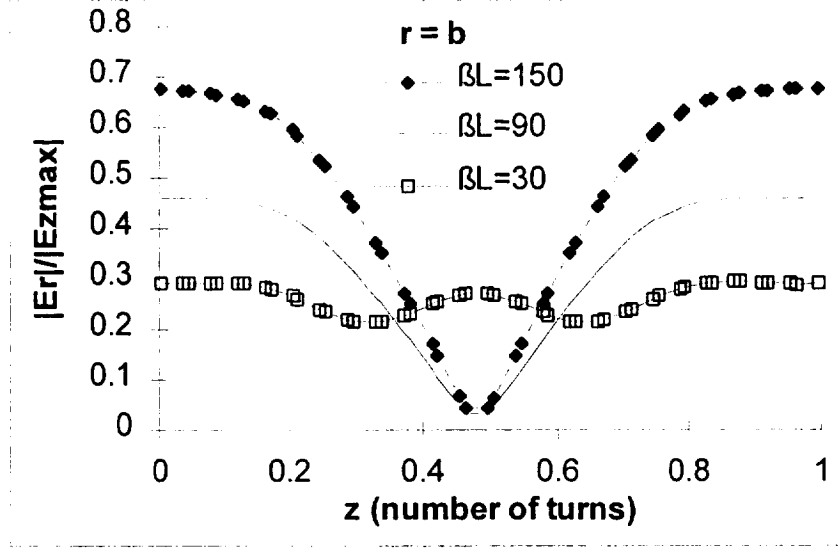


Figure 3 Radial electric field amplitude normalized to the maximum value of longitudinal electric field as a function of z at $r=b$ and $\theta = 0$

The general relationship

$$P = w v_g \quad \text{Equation 1}$$

is used where P is time averaged RF power flow, v_g is group velocity and w is time averaged stored electromagnetic energy per unit length. The group velocity can be calculated from the dispersion curve obtained using MAFIA [13]. Assuming a constant pitch to simplify the calculations, K_0 and v_g will be the same for the simulated circuit and at the output of the actual tube. The change in pitch when a velocity taper is implemented will cause K_0 and v_g to vary slightly, but we neglect this variation here. The respective relationships for RF power flow can be expressed as

$$\begin{aligned} P_{out} &= w_{out} v_g \\ P_{MAF} &= w_{MAF} v_g \end{aligned} \quad \text{Equation 2}$$

The RF power flow at the output of the actual tube P_{out} is given in Table I. The RF power flow in the simulated circuit P_{MAF} can be calculated from (1) as the energy, w_{MAF} , is calculated directly by the code. Therefore, energy at the output of the tube can easily be determined and expressed in terms of simulation energy by a scale factor A_{out} , or

$$w_{out} = A_{out} w_{MAF} \quad \text{Equation 3}$$

The stored electromagnetic energy per unit length is proportional to the electric field squared integrated over the circuit volume, or

$$\begin{aligned}
W_{out} &\sim \varepsilon \int_{vol} E_{out}^2 dv \\
W_{MAF} &\sim \varepsilon \int_{vol} E_{MAF}^2 dv
\end{aligned}
\tag{Equation 4}$$

where E_{out} and E_{MAF} designate total RF electric field at the output of the tube and for the simulated circuit, respectively. If the energy differs by a scale factor this leads to

$$E_{out}^2 = A_{out} E_{MAF}^2 . \tag{Equation 5}$$

So that

$$E_{out} = \sqrt{A_{out}} E_{MAF} . \tag{Equation 6}$$

Thus, the magnitude of electric fields obtained using MAFIA can easily scale to be commensurate with values that are present at the output of the experimental tube. Using appropriate values from the experimental tube listed in Table I, electric field values at 26 GHz and at the beam radius were calculated for the output of the 8916H TWT as shown in Table II. It should be noted that the MAFIA fields are calculated in the absence of a beam, but the electron beam will have a relative permittivity slightly less than one, thus perturbation on actual RF fields due to the beam will be minimal.

In order to compare the forces due to the RF electric fields at the output of the tube to space charge forces, the radial space charge field is calculated at the boundary of a beam having a circular cross section and radius b as [14]

$$E_{rsc} = -\frac{I_o}{2\pi b \varepsilon_o \mu_o} \tag{Equation 7}$$

where I_o is the beam current, and ε_o and μ_o are the free space permittivity and permeability, respectively. Assuming a beam radius to helical average radius ratio of 0.5, the scaled values of the electric field at the output are normalized to this value of space charge field in Table II. Radial, azimuthal and axial electric fields at the output reach 61%, 26% and 132% of the space charge field, respectively. Since the force on a charge q to an electric field E can be expressed as $F = -qE$, the forces from the RF fields will amount to the same percentages compared to space charge forces. The significance of these forces indicates the importance of including these fields in helical TWT beam focusing design codes. From Figure 2 and Figure 3 it can be seen that radial and azimuthal components of electric field become stronger with respect to the longitudinal component as the frequency is increased. Thus, the effect of RF fields on beam optical properties will be more significant with increasing frequency. Additionally, it is well known that the strength of transverse RF components in a helical circuit increases with radius indicating more of an effect with larger beam radius as well.

Table II Scaled MAFIA RF Electric Field Values at 26 GHz and $r=a/2=b$

| Component | Scaled to Output (V/m) | E_{RF} / E_{rsc} at Output |
|------------|---------------------------|---------------------------------|
| E_r | 97,364 | 0.61 |
| E_θ | 42,394 | 0.26 |
| E_z | 211,969 | 1.32 |

CONCLUSION

The advent of an accurate 3D helical TWT slow-wave circuit model allowed for calculation of RF field forces and comparison to radial space charge forces showing a significant contribution. The forces due to radial, azimuthal and axial electric fields at the tube output reach 61%, 26% and 132% of space charge forces, respectively, at 26 GHz for the device studied. This effect is expected to increase with frequency and beam diameter. These results can be generalized to indicate implementation of RF field effects in beam optics codes, particularly near the output of the tube, could provide meaningful insight allowing improved beam-focusing designs by reducing beam-circuit interception. In addition, most TWT interaction codes such as [15] neglect the azimuthal component of RF electric field, and often the spent beam data from these interaction codes are used as the basis of collector design. Existence of the azimuthal electric field component, however, will increase the transverse energy of the electron beam and modify this spent beam behavior. Thus, including transverse RF field effects could aid in optimal multistage depressed collector design.

A more quantitative study is being completed using the 3D particle-in-cell solver of MAFIA to determine how RF fields affect beam characteristics such as radius, scallop, ripple, percent transmission and tunnel emittance as a function of length and frequency.

BIBLIOGRAPHY

-
- 1 C. L. Kory and J. A. Dayton, Jr., Accurate Cold-Test Model Of Helical TWT Slow-Wave Circuits, *IEEE Trans. on Electron Devices*, Vol. 45, No. 4, pp. 966-971, April 1998.
 2. T. Weiland: On the Numerical Solution of Maxwell's Equations and Applications in the Field of Accelerator Physics, Part. *Accel.*, vol 15, pp. 245-292, 1984.
 3. T. Weiland: On the Unique Numerical Solution of Maxwellian Eigenvalue Problems in Three Dimensions, Part. *Accel.*, vol. 17, pp. 227-242, 1985.
 - 4 R. P. Lagerstrom, Interaction impedance measurements by perturbation of traveling waves, Stanford Electronics Laboratories Technical Report No. 7, February 11, 1957.
 - 5 C. L. Kory and J. A. Dayton, Jr., Computational Investigation of Experimental Interaction Impedance Obtained by Perturbation for Helical Traveling-Wave Tube Structures, *IEEE Trans. on Electron Devices*, Vol. 45, No. 9, pp. 2063-2071, September, 1998.
 - 6 Personal communication with Will Menninger of Hughes Aircraft Co., Electron Dynamics Division.
 - 7 R. Berterottier, "Focalisation magnétique dans un faisceau de révolution modulé en densité, *Ann D. Radioelec*, vol. 4, pp. 289-294, October, 1949.
 - 8 W. W. Rigrod and J. A. Lewis, Wave propagation along a magnetically focused cylindrical electron beam, *Bell Syst. Tech. J.*, vol. 33, pp. 399-416, March, 1954.
 - 9 G.R. Brewer, Some effects of magnetic field strength on space-charge-wave propagation, *Proc. IRE*, vol.44, pp.896-903, July, 1956.
 - 10 G. R. Brewer and J. R. Anderson, Electron-Beam Defocusing due to high-intensity RF fields, *IRE Trans. on Electron Devices*, vol. 8, no. 6, 1961.

11 R. L. Bell and M. Hillier, An 8-mm klystron oscillator, Proc. IRE, vol. 44, pp. 1155-1159, September, 1956

12 O. T. Purl, J. R. Anderson and G. R. Brewer, A High-Power Periodically Focused Traveling-Wave Tube, Proceedings of the IRE, February 1957, pp. 441-448

13 Kory, C. L.; Wilson, J. D.: Three-Dimensional Simulation of Traveling-Wave Tube Cold-Test Characteristics Using MAFIA, *NASA TP-3513*, May 1995.

14 A. S. Gilmour, Jr., *Principles of Traveling-Wave Tubes*, Norwood, MA: Artech House, 1994.

15 H. K. Detweiler, Characteristics of magnetically focused large-signal traveling-wave amplifiers, Rome Air Development Center Tech. Rep. RADC-TR-68-433, Griffiss Air Force Base, NY, 1968.

